Available online at www.sciencedirect.com

ScienceDirect

Current Opinion in
Colloid & Interface Science

Small-angle X-Ray and neutron scattering in food colloids

Elliot Paul Gilbert[1,2]

Abstract

Small-angle and ultra-small-angle X-ray and neutron scattering techniques provide structural information on the nanometre-to-micron length scale. This review describes recent examples and advances of these techniques in the field of food colloids. The article highlights the structural information that can be extracted when applied to all macronutrient classes, namely fats, carbohydrates and proteins, and mixtures thereof, as well as covering emerging applications and future opportunities.

Addresses

[1] Australian Centre for Neutron Scattering, ANSTO, New Illawarra Road, Lucas Heights, NSW 2234, Australia

[2] The Australian Institute for Bioengineering and Nanotechnology and Queensland Alliance for Agriculture and Food Innovation, The University of Queensland, Brisbane, QLD 4072, Australia

Corresponding author: Gilbert, Elliot Paul (elliot.gilbert@ansto.gov.au)

Current Opinion in Colloid & Interface Science 2019, **42**:55–72

This review comes from a themed issue on **X-Ray and Neutron Scattering**

Edited by **Jeff Penfold** and **Norman J. Wagner**

For a complete overview see the Issue and the Editorial

https://doi.org/10.1016/j.cocis.2019.03.005

Introduction

Whether we consider individual ingredients or whole products, food is essentially a mixture of components with structure on multiple length scales (from atomic to visible) that can exist in various physical states with different extents of mobility (translation, rotation and vibration). Food colloids may exhibit properties that are both liquid-like and solid-like, and this behaviour is often time dependent. Metastable structures can also be attained because they are favoured kinetically. As Aguilera and Lillford [1] note, food materials can exist as "non-equilibrium structures stabilised by relatively weak forces. As engineered structures, they are 'poor' because they change appreciably with time". Such behaviour is apparent in the induction period in lipid crystallisation, relaxation in freeze-dried protein powders or the influence of processing conditions on digestion kinetics. It is the combination of the attributes of structure, motion and response to external stressors (e.g. temperature, pressure and shear) that informs the suitability of a given ingredient, how a food can be developed (e.g. processing) and the extent to which the product meets a specific need (e.g. nutritional, sensorial and consumer-driven). All of these factors are relevant to food colloids.

Although small-angle scattering (SAS) methods are extremely powerful, providing structural information on the nanometre-to-micron length scale, they are never sufficient in their own right to 'understand' material structure; an array of complementary characterisation techniques is essential to explore the relevant size and, indeed, time scales. This is even more so in the case of food systems that comprise diverse components, and in various forms, including suspensions, gels, foams and emulsions, and whose physics have been described in the excellent review by Vilgis [2]. However, small-angle scattering represents a critically important characterisation technique to probe food structure on a highly relevant length-scale yielding system details unavailable from other approaches.

Although inevitably not exhaustive, this review summarises the latest activities in the application of SAS to food colloids, limited to outputs from the last three years. However, in some cases, where a field can be placed into a broader context, for example, where an appropriate review exists, this has been included. The abbreviations small-angle neutron scattering (SANS), small-angle X-ray scattering (SAXS) or SAS will be used where neutron, X-ray or both radiation sources have been used in a study; for ultra-SAS techniques, ultra-small-angle neutron scattering (USANS), ultra-small-angle X-ray scattering (USAXS) or ultra-small-angle scattering (USAS) will be used accordingly. Considerable thought has been given to the most logical order for presentation, for example, based on form (e.g. solution, suspension, emulsion, gel) or by product (dairy, meat, plant, beverage); however, neither of the options was ultimately satisfactory. Instead, the choice has been made here to demarcate according to macronutrient class (lipid, carbohydrate, protein).

Small-angle X-ray and neutron scattering

Owing to an inverse relationship, the scattering of X-rays and neutrons at 'small' q, defined below, gives rise to structural details over 'larger' (than atomic) length scales, from approximately one to several hundred nanometres and extending to microns in the case of USAS methods; for materials science application, SAS and USAS are, therefore, defined to be 'large-scale' structural probes. On this size range, the technique is sensitive to the arrangement of assemblies of atoms enabling molecular structure and spatial distribution to be determined. There are multiple tomes on SAS, and only the necessary basics are described here. For further information, the reader is encouraged to consult the SAS Portal [3] which has a useful list of resources including recommended books, journal articles, web-based tools, blogs and primers.

A small-angle scattering experiment conventionally measures the intensity of scattered radiation versus the magnitude of the scattering vector q; the latter equates to $(4\pi/\lambda)\sin\theta$, where 2θ is the scattering angle and λ is the wavelength of the incident radiation. A typical SAS geometry is shown in Figure 1a; to reach lower q and access information on larger length scales, USAS instruments are used which typically use a Bonse–Hart double-crystal geometry to provide sufficient angular resolution. The measured intensity may be written as follows: $I(q) = \frac{d\Sigma}{d\Omega}(q) = (\Delta\rho)^2 V_p^2 N_P P(q) S(q)$, where $d\Sigma/d\Omega(q)$ is the differential scattering cross-section, $\Delta\rho$ is the scattering contrast between the species of interest and its surroundings, V_p is the volume and N_p the number of species per unit volume. $d\Sigma/d\Omega(q)$ contains all the information regarding the size, shape and interactions between the scattering species in the sample where the form factor, P(q), describes the scattering from an individual scattering species and the structure factor, S(q), describes the scattering between scattering centres. For isotropic scatterers, data are typically radially averaged—the most common case for food colloids—unless preferred orientation exists in the system of interest (e.g. under flow or deformation).

For SAS to occur, there must be a contrast between the species of interest and its surroundings. The scattering contrast, $\Delta\rho$, is equal to $\Delta\rho = \rho_p - \rho_m$, where ρ_p and ρ_m are the scattering length densities (SLDs) of the species of interest and solution or surrounding matrix, respectively. The SLD, ρ, of a molecule with i atoms can be calculated from $\delta N_A \Sigma b_i/M$, where δ is the bulk physical density of the molecule (gcm^{-3}), N_A is Avogadro's number, b_i is the X-ray or neutron, as appropriate, scattering length of the ith atom in the molecule and M is the molecular weight. Thus, the contrast may be simply calculated from knowledge of the physical density of the molecule and its atomic composition. Contrast is radiation source dependent, the X-ray

Figure 1

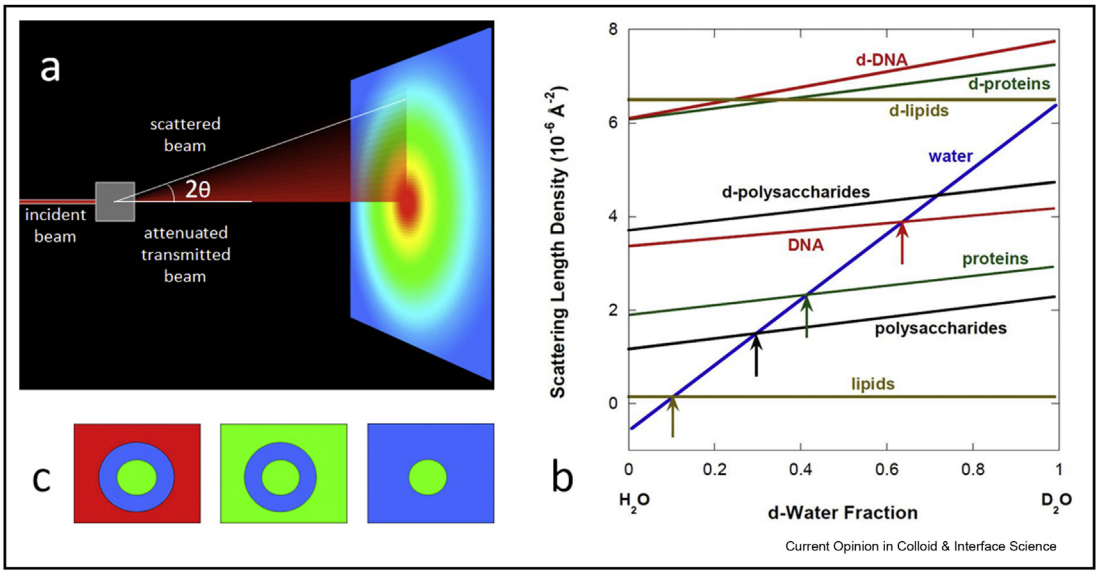

The basics of small-angle scattering in food colloids. **(a)** Scattering geometry for a SAXS or SANS measurement; **(b)** Neutron scattering length densities for common food-based materials (after Hammouda [4]); **(c)** Core-shell nanostructure in solution showing the possibility of selectively contrast matching either of the phases through changing solvent H_2O/D_2O composition: by matching the SLD of the solvent to core, only the shell is visible, while matching the solvent to the shell yields information only on the core. Reprinted from Trends in Food Science and Technology 20, Amparo Lopez-Rubio and Elliot Paul Gilbert, Neutron Scattering: A Natural Tool for Food Science and Technology Research, 576–586, Copyright (2009), with permission from Elsevier [5]. SLD, scattering length density; SANS, small-angle neutron scattering; SAXS, small-angle X-ray scattering.

scattering length is determined by the number of electrons, whereas the neutron scattering length is determined by the structure of the atomic nucleus; consequently, SAXS and SANS provide complementary information. Contrast can be manipulated through 'contrast variation' which, in the context of SANS in food colloids, relies on the different neutron scattering lengths of hydrogen and deuterium. As the SLD for H_2O is negative and for D_2O is positive, components may be strategically contrast matched using mixtures of heavy and light water so that they effectively become transparent to neutrons (Figure 1b); this greatly simplifies the scattering contributions in multicomponent systems as is shown Figure 1c for a model core–shell particle with regions of different SLDs. Contrast variation may also be achieved through intrinsic differences in chemical composition and physical density or via strategic selective deuteration (e.g. replacement of hydrogen with deuterium in a fatty acid). X-ray solvent contrast can be manipulated using sucrose, glycerol or salts, while anomalous SAXS (ASAXS) and resonant soft X-ray scattering (RSoXS) involve varying the X-ray energy across the absorption edge of a relevant element where the wavelength dependence of the atomic scattering length is significant.

It is advantageous to conduct measurements as close as possible to the 'native' state of a material, that is, under relevant environmental conditions. In this sense, SAS possesses particularly attractive attributes for food colloids as, except in some cases where synchrotron X-rays are used, SAS constitutes a non-invasive technique, enabling the study of partially hydrated materials, gels and solutions. The lack of special sample preparation, for example, staining, also naturally leads to a minimisation of possible sample artefacts. However, unlike microscopy techniques, SAS yields non-visual information providing structural information in 'reciprocal space'. This means that scattering data have to be either inverted back to real space or fitted with reciprocal space models. Unquestionably, this has been a barrier to greater uptake within the food materials science community. If data are collected over a sufficiently wide q range, Fourier transformation to generate a distance distribution function, P(r), is possible in the case of dilute scatterers; this approach provides information not only on the spatial extent of the particle but also its shape and is commonly used in the study of protein solutions. One-dimensional correlation functions can be used to extract information on lamellar structures, for example, starch. If data are fitted to models describing structures in reciprocal space, mathematical functions are required whose parameters must be based on existing knowledge of the system; it is, therefore, essential that information obtained from complementary techniques is available. Conducting SAS measurements with multiple contrasts (contrast variation SANS or ASAXS) serves to provide additional constraints to reduce the number of possible models. Mathematical form factors have been developed for many scattering symmetries and applied to, for example, polysaccharide solutions. These form factors can be combined with a range of structure factors to describe interparticle interactions and separation, the latter giving rise to diffraction peaks (for example, for lipids or starch). Occasionally, models are not strictly required, and some structural parameters can be extracted from data in a straightforward manner, for example, Guinier or Porod analysis and in systems exhibiting fractal behaviour. Further information on such approaches can be found in [3] and [4].

Lipids

Crystallisation and aggregation of fats and oils

Chemically, fats consist chiefly of triglyceride (TAG) molecules composed of a glycerol backbone onto which three fatty acid moieties are esterified. Depending on the degree of saturation of the fatty acids, it will behave either as a solid (fat) or liquid (oil) at different temperatures and, in many food applications, some edible fats may exist as a supersaturated solution of high-melting TAGs in an oil of liquid TAGs. Fat crystals display polymorphic behaviour which also affects melting behaviour; the more stable the polymorph, the greater the TAG packing density leading to greater melting point and enthalpy. In order of increasing stability, they exhibit hexagonal, orthorhombic and triclinic subcell packing, commonly known as α, β' and β polymorphs, respectively. Relevant to the SAS region, TAGs can pack into lamellae with double (2L) or triple (3L) chain length structure. On a larger length scale, crystalline nanoplatelets (CNPs) can form whose size and shape depend on composition as well as processing conditions [6]. The Marangoni group at the University of Guelph have been using SAS and USAXS to explore the hierarchical crystallisation behaviour of TAGs with an aim towards improving the functional properties of fats and fat-containing products (Figure 2) [6,7].

CNPs can be modified through the control of chemical composition (including degree of saturation), cooling rate, extent of supersaturation and external shear fields. CNPs may form stacks whose size can be determined by applying the Scherrer equation to the SAXS lamellar peak. In turn, CNPs can aggregate via attractive van der Waals interactions to form polycrystalline clusters which can then further aggregate to form a fat crystal network. Liquid oil, trapped within the system, presents challenges for using electron microscopy, making scattering methods particularly attractive. CNPs may exhibit more laterally organised structures such as cylindrical aggregates dubbed "TAGwoods"; the latter is a reference to the multilayered sandwich of favour for Dagwood, a central character in the comic strip Blondie. Combinations of scattering and fluid simulation have been

Figure 2

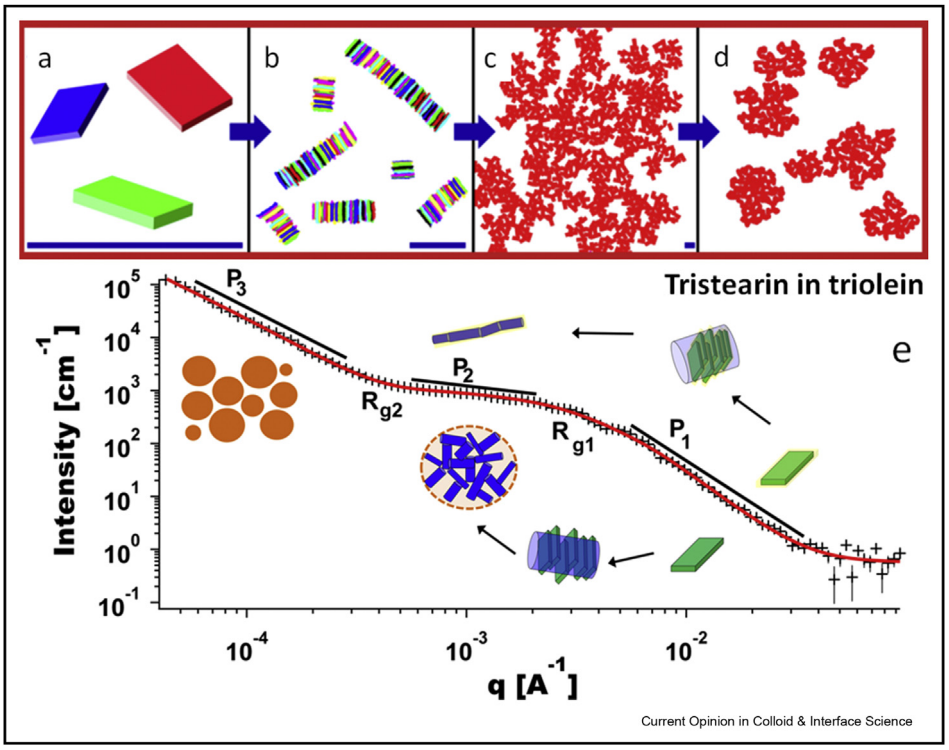

Hierarchical structures in triglycerides. **(a–d)** Computer simulation predictions **(e)** USAXS intensity data for a static system of 20% (w/w) tristearin (solid) in triolein (liquid) oil. (a) Model CNPs (D = 2). (b) Aggregation into TAGwoods (D = 1). (c) TAGwood aggregation via Diffusion/Reaction-Limited Cluster Aggregation (D = 1.7–2.1). (d) Uniformly distributed TAGwood clusters (D = 3). D is the fractal dimension. The horizontal line indicates the same length (approximately 1000 nm) on the different length scales. For short-time observations (fast cooling followed immediately by X-ray scattering), (a) and (b) will be observed with a random distribution (D = 3) of TAGwoods. For long-time observations, (a–d) will be observed. (e) USAXS data after cooling at $1^{\circ}Cmin^{-1}$ to ~23 °C with the structures identified. P_i (i = 1, 2, 3) and R_{gi} (I = 1, 2) are Porod and Guinier exponents in a unified model fit. Figure courtesy of Alejandro Marangoni. CNP, crystalline nanoplatelet; USAXS, ultra-small-angle X-ray scattering.

applied to investigate the influence of shear rate on the formation of fat crystal networks [8].

Given the above complexity, it would be advantageous, particularly for industrial processing, to be able to decouple fat crystallisation and network formation. Indeed, in the formation of fat-continuous food emulsions, fat crystallisation and network formation occur simultaneously with emulsification. Some control and predictability can be achieved using precrystallised fat nanoplatelets which offer simplified formulation and processing routes for low-fat food products. A fine powder of rapidly micronised fat crystal (MFC) nanoplatelets can be produced by taking a saturated molten fat blended with supercritical CO_2 that is rapidly expanded through a nozzle; the latter can be readily dispersed in oil. Nikolaeva et al. investigated untreated and melt-cooled MPCs in sunflower oil after storage, as a function of concentration and shear using USAXS, SAXS, rheo-SAXS and WAXS, rheo-MRI and Raman imaging [9]. During network formation, the rough MFC surfaces impede stacking interactions and the formation of TAGwoods. The application of shear does not affect the size of the MFC aggregates but does induce the release of nanoplatelets from the weakly connected continuous network and subsequent alignment along the flow direction. They find that the network grown under static conditions is metastable; under shear, rapid recrystallisation of thinner nanoplatelets occurs.

Low-melting-point oils in food sometimes crystallise during chilling and/or freezing, often causing deterioration in the sensorial properties of food emulsions as well as promoting fat oxidation. In this context, Miyagawa et al. [10] studied the crystallisation behaviour of rapeseed oil, whose major components are oleic, linoleic and linolenic acid, to better understand and control the structure and kinetics of crystallisation. After a certain induction period, following cooling and under isothermal storage, metastable crystal structures are observed which can be detected in SAXS/WAXS as well as differential scanning calorimetry (DSC). The crystallisation behaviour differs with storage temperature but not cooling rate, with 3L transforming to 2L crystals for −17 and −20°C but maintained at −25°C. Similarly, the crystalline structure of anhydrous milk fat has been

investigated as a function of temperature, complemented by non-simultaneous Raman spectroscopy and DSC [11]. Two TAGs are present, one in α form with 3L lamellar organisation and a second organised in the more stable β′ form with 2L structure. Using the characteristic diffraction peaks, the most probable structures formed on either cooling or heating anhydrous milk fat are proposed. Larger length-scale structures have been revealed with scanning electron microscopy (SEM) and USAXS but with different crystallisation behaviour where only the 2L structure is observed although the latter may be due to differences in purification [12].

Phytosterols are found in cereals, nuts, vegetables and fruit. Their chemical similarity to human cholesterol enables phytosterols to reduce serum cholesterol by preventing its absorption in the intestinal tract as a result of competitive solubilisation into the bile salt micelles; this, in turn, results in an increase in endogenous cholesterol synthesis and removal of low-density lipoprotein (LDL) in the blood. However, to achieve sufficient sterol consumption for LDL reduction, dietary supplementation is needed with emulsion-based delivery providing one such approach. Zychowski et al. [13] investigated oil-in-water (O/W) emulsions stabilised by whey protein isolate, as potential phytosterol delivery vehicles, in which the oil phase comprised a mixture of crystalline phytosterols with anhydrous milk fat. SAXS diffraction peaks demonstrated that phytosterol can integrate within the milk fat TAG matrix in the expected 3L structure, albeit within an increase in longitudinal packing and system disorder.

Fish oils are recommended for a healthy diet due to their high content of ω-3 fatty acids; the latter have been proposed to provide benefits against cancer, cardiovascular diseases, cognitive decline, inflammation and depression. However, fortification of ω-3 fatty acids into food products is a challenge as fish oils are highly susceptible to lipid oxidation, leading to rancid off-flavours and potentially toxic reaction products. Truong et al. [14] showed that fish oil oxidation can be reduced through the addition of the solid fraction of anhydrous milk fat. SAXS verified the expected double and triple lamellar structures of tristearin with WAXS showing α, β' and β polymorphs. Such studies may be relevant in developing solid lipid nanoparticles for encapsulation.

Milk fat globules have a broad size distribution (1–20 μm) and an average size of about 3 μm. The globules are surrounded by the milk fat globule membrane composed of polar lipids; of which, sphingomyelin (SM) accounts for up to 45 wt%. Noting that SM itself, contains a variety of molecular species, Lopez et al. [15] performed simultaneous synchrotron SAXS/XRD (X-ray diffraction) and DSC to investigate the phase behaviour of milk–SM and milk–SM/cholesterol mixtures. Reflecting the complexity of the system, they identified a conversion from a fully interdigitated to mixed interdigitated lamellar structure which subsequently transitioned into a liquid crystal phase. Cholesterol induces increased organisation of the milk–SM bilayers, with the formation of a liquid-ordered lamellar phase. The knowledge gained has relevance to many mechanisms occurring in the gastrointestinal tract, that is, milk fat globule digestion, immunity and maturity of the intestine.

SANS has been used to probe the structure of the Italian liquor Limoncello [16]; it is a complex colloidal system, made of essential oils from lemon with ethanol, sucrose and water. Samples were prepared from lemon peel, macerated in deuterated ethanol with sucrose syrup prepared in deuterated water, to enable appropriate neutron contrast of oil with respect to the other components. The system is composed of polydisperse oil droplets dispersed in a continuous water/ethanol/sucrose phase whose interfacial area can be determined through Porod analysis and whose size distribution can be fitted with a polydisperse sphere model. The droplets, whose mean size is ca. 100 nm, show little variation with temperature and overall ternary solvent composition and are in equilibrium with molecularly dissolved oil. At a system composition close to that of commercially available Limoncello, approximately one third of the oil is molecularly dissolved and is in equilibrium with the submicron droplets. The authors propose that the observed structures formed have a direct impact to sensory properties.

Lipid self-assembly

Lipid self-assembled structures are ubiquitous in colloids, but within the food (as well as the pharmaceutical) industry, they are particularly relevant in the context of targeted delivery and reactivity control. Mixtures of two of the most abundant emulsifiers available—phospholipids (of which, lecithin is the most widely used in the food industry) and monoglycerides—form a diverse array of structures: micelles, vesicles, reverse microemulsion and lyotropic liquid crystalline phases comprising inverse micellar cubic, inverse hexagonal (H_2) and inverse bicontinuous cubic phases. Sagalowicz et al. [17] review their application for reactivity control in food and note that such structures can increase the solubilisation of lipophilic and crystalline materials, increase the bioavailability and bioefficacy of drugs and nutrients and the controlled release of solubilised bioactive materials. SAS is inevitably one of the techniques of choice to evaluate the structural diversity in such systems. Structure modulation can also be used to tune oil oxidation kinetics as well as aroma, taste and colour via the amino acid–reducing sugar (Maillard) reaction. The effects of unsaturation degree and fatty acyl chain length on the self-assembled structures formed by the ω-3 polyunsaturated fatty acid monoglycerides, docosahexaenoic

acid, docosapentaenoic acid and eicosapentaenoic acid monoglycerides have been studied with SAXS [18,19]; they form a dominant H_2 phase in excess water at 25°C and a temperature-triggered structural transition to an inverse micellar (L_2) phase. By adding the food-grade emulsifier CITREM (an anionic citric acid ester of monoglycerides and diglycerides made from sunflower oil), the resulting hexosome nanoparticles have been studied as potential nanocarriers for delivering nutritional compounds or drugs. Increasing unsaturation degree is associated with a significant decrease in the corresponding H_2 phase lattice parameter and a reduction in the H_2—L_2 phase transition temperature. These systems have also been investigated when formed using microfluidics, combined with synchrotron SAXS [20]. Curcumin is a hydrophobic phytopolyphenol found in turmeric which has been promoted for antioxidant, anti-inflammatory, antimicrobial and anticancer properties. The release kinetics of curcumin as a function of composition have been studied from an H_2 liquid crystalline system [21]. Fonseca-Santos et al. [22] explored the use of nonionic lamellar liquid crystalline systems for controlled delivery of resveratrol, a poorly aqueous soluble molecule found in grape skin, peanuts and red wine and attributed to have anti-inflammatory activity.

Lipid digestion

The digestion of triglycerides in the human digestive tract results in the conversion of water-insoluble molecules into more polar products—amphiphilic sn-2 monoglycerides and two free fatty acids—that can be absorbed into the circulatory system. SAS has been used widely to investigate the cascade of colloidal structures formed during simulated digestion, relevant both to nutrient uptake from food as well as drug delivery. However, differences in opinion exist as to the most suitable chemical components that most appropriately mimic the complex conditions in the gastrointestinal tract. Human intestinal fluids comprise a complex mixture of bile salts, phospholipids, steroids and glycerides that vary in composition in the fed and fasted state and between subjects. Clulow et al. [23] used SAXS, as well as cryo-TEM (transmission electron microscopy) and molecular dynamics, to show that not all simulated intestinal fluids (SIFs) are created equal. In-house prepared SIFs based on sodium taurodeoxycholate and 1,2-dioleoyl-sn-glycero-3-phosphatidylcholine were shown to form monodisperse oblate ellipsoidal micelles irrespective of lipid concentration and preparation conditions. In contrast, commercially available SIFs based on sodium taurocholate and lecithin formed different, polydisperse, colloidal structures in the fed and fasted states, namely prolate ellipsoidal micelles and vesicles, respectively. They demonstrate that sodium taurodeoxycholate and 1,2-dioleoyl-sn-glycero-3-phosphatidylcholine micelles are more suitable candidates for standardising SIF formulations. Rezhdo et al. [24] used contrast variation SANS to investigate the change in dimensions of bile salt micelles during lipolysis of triolein or due to the presence of digestion products. It is noted that model fits suggest polydispersities of the order of 45%; the use of methanol in mixtures used to terminate digestion may also have influenced the structures observed.

Self-assembled lipid nanostructures formed during digestion may be suitable as oral delivery vehicles for poorly water-soluble bioactive food components such as carotenes, vitamins A, D, E and K, as well as drugs, particularly under compromised bile salt conditions. Taking advice from Hippocrates who said “Let food be thy medicine and medicine be thy food”, the Boyd group at Monash University have focussed attention on milk as an enhanced drug delivery vehicle. Using time-resolved synchrotron SAXS, they compared the structure of a suspension of the crystalline antimalarial drug artefenomel (OZ439) in milk, in the presence and absence of lipase. The colloidal structures formed during milk digestion resulted in dissolution of the free-base form of the drug and recrystallisation into a more stable polymorphic form as well as a significant reduction in crystalline OZ439 overall. Such behaviour was only observed when both milk and lipase were present. Milk may, therefore, be particularly suitable as a form of lipid-based formulation for coadministration with OZ439, from which both an enhancement in OZ439 oral bioavailability and delivery of nutrients should result. Similar studies have been conducted with halofantrine, which has a close structural relationship to lumefantrine, an antimalarial drug of current interest for the treatment of paediatric malaria [25]. While formulations based on milk face significant challenges in a regulatory sense, there are opportunities for product development using the major triglycerides constituting milk or highly regulated milk powders. In a follow-up study, the extent to which milk tablet formulations can be used to improve solubilisation of poorly water-soluble drugs was explored [26]. Using either freeze-dried bovine milk or infant formula, the release of cinnarizine was studied with synchrotron SAXS. Tableting had a significant impact on the self-assembly of lipids in redispersed milk tablets, whereas no effect was seen for infant formula tablets. Incorporation of a disintegrant to reduce tablet dispersion times promoted the formation of hexagonal liquid crystalline phases upon digestion but had minimal effect on drug solubilisation. Clulow et al. [27] probed the robustness of the kinetic structural behaviour when milk is subjected to homogenisation, lyophilisation, freeze-thawing and freeze-drying, that is, the range of processes typically encountered or that are relevant to the use of milk in pharmaceutical applications (Figure 3).

Mayonnaise is an O/W emulsion, consisting of egg—lecithin—stabilised oil droplets that contain up to 80%

Figure 3

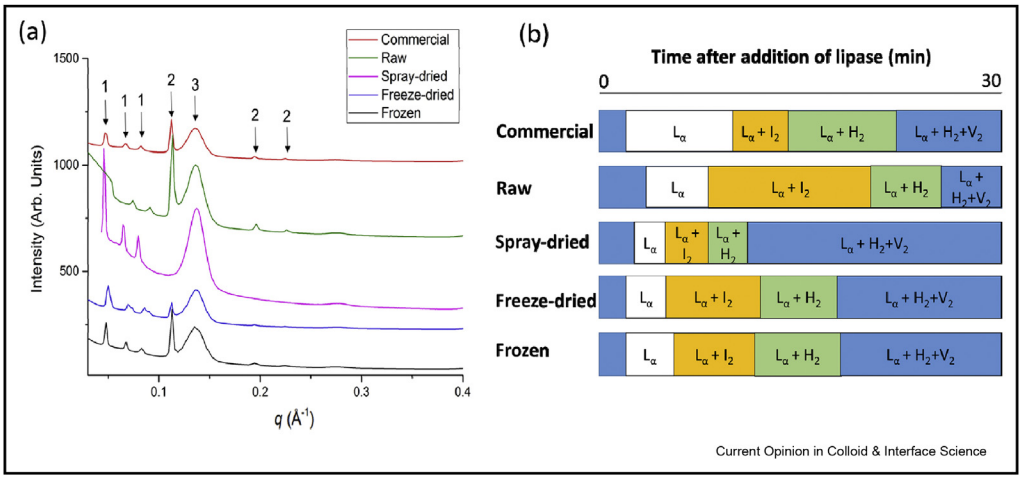

Digestion of bovine milk studied with SAXS. **(a)** SAXS patterns of commercial (homogenised and pasteurised) milk, raw milk, spray-dried commercial milk, freeze-dried commercial milk and pre-frozen commercial milk after 30 min digestion at pH 6.5, 37 °C. The bicontinuous cubic phase Im3m is annotated as '1′, the inverse hexagonal phase H_2 as '2′ and the lamellar phase L_α as '3'. **(b)** Schematic representation of the timing of phase transitions during digestion of milk from different sources; I_2 is the inverse micellar cubic Fd3m phase, and V_2 is the inverse bicontinuous cubic Im3m phase. Reprinted from Chemistry and Physics of Lipids 211, Clulow AJ, Salim M, Hawley A, Boyd BJ., A closer look at the behaviour of milk lipids during digestion, 107–116, Copyright (2018), with permission from Elsevier [27]. SAXS, small-angle X-ray scattering.

vegetable oil TAGs. Similar to the aforementioned studies, time-resolved synchrotron SAXS conducted under simulated *in vivo* conditions during the digestion of mayonnaise combined with gradual pH increase from pH 6.5 to 7.4 revealed that highly ordered nanostructures are formed inside mayonnaise emulsion droplets [28]. While structural transitions occur at constant pH, an increase in pH during lipolysis promotes the transformation of the hydrophobic oil environment inside the mayonnaise emulsion droplet to highly organised hydrophilic interfaces and vesicles as final structures via the formation of emulsified microemulsions, a micellar cubic Fd3m phase, an H_2 phase, Pn3m-type cubosomes and a sponge (L_3) phase.

Oleogels

Driven by consumer demand and government regulation, there is a major impetus within the food industry to replace traditional edible *trans* and saturated fats with 'healthier' alternatives, typically unsaturated or polyunsaturated fats. However, saturated fats with their higher melting temperature impart texture and pleasurable mouthfeel to products. The replacement of solid fats, therefore, leads to formulation challenges to provide appropriate structuring, while maintaining positive consumer perception and acceptance. One such approach is to incorporate gelator molecules into liquid oil systems to form organogels. For food applications, the prefix organo- is replaced by oleo-. Oleogelation can be achieved using phytosterols, phospholipids, vegetable waxes, monoglycerides or diglycerides, which structure into a 3D network that can entrap oil. The gelling ability is naturally related to the balance between the soluble and insoluble fractions of the gelator in the solvent; the molecule must be relatively insoluble to self-assemble into anisotropic structures but with a soluble fraction to interact with the oil moieties. The composition of the oleogel will thus differ depending on the means of gelation, and by changing the gelator concentration, it is possible to tune properties, such as the hardness and melting point of the gel, to suit the desired application. The effect is liquid oils being structured and gelled by nontriglyceride networks to take on solid-like properties.

SAXS, as well as rheological measurements, DSC and polarised microscopy have been applied to investigate the influence of oil and gelator on oleogel properties using four food-grade gelators with different hydrophilic heads (glyceryl and sorbitan) and hydrophobic tails (monostearic or tristearic chains) in medium- (MCT) and long-chain triglyceride (LCT) oils [29,30]. Lamellar diffraction peaks are observed in the SAXS in all cases with power law exponents between −2 and −3. As expected, gel properties increase with gelator concentration but not linearly and reach a threshold beyond which steric effects dominate. Glyceryl-based gelators produce the most structured oleogels, whereas monostearate leads to the formation of stronger oleogels with greater lamellar spacing. Oleogels produced with LCT are stronger and gel at lower concentration than MCT. Beeswax—a complex mixture of mostly straight-chain monohydric alcohol compounds and straight-chain acids—is used as a glazing and coating agent, a

texturizer for chewing gum base, a carrier for additives but also as a gelator. Relevant to bioactive-compound delivery, Martins et al. [31] showed that oleogels formed with increasing beeswax concentration were stronger and increasingly effective in enhancing oxidative stability of β-carotene [32]. Lecithin oleogels have limited potential for food application due to their sensitivity to water; however, lecithin has been considered as a co-oleogelator to tune the self-assembly of host structuring agents. Okuro et al. [33] explored its effect on phytosterol-based oloeogels formed with MCT, sunflower oil or hexadecane with SAXS, DSC, rheology and optical microscopy.

Oleosomes

Oleosomes are oil bodies formed in oleaginous plants representing lipid reservoirs surrounded by a continuous monolayer of phospholipids and proteins. Their sizes range from several hundred nanometres (e.g. soy beans) up to a few micrometres (e.g. cocoa). They have a wide range of applications in the food and cosmetics industries, including as natural emulsifiers, foaming agents or encapsulation matrices for hydrophobic compounds. Contrast variation SANS has been used to separate contributions from the lipid and protein components to the core–shell form factor scattering as well as exploring the structure of pectin-encapsulated oleosomes as a function of heat treatment [34].

Carbohydrates

Carbohydrates can be classified into monosaccharides, oligosaccharides and polysaccharides. Polysaccharides account for more than 90% of the dry content of fruit and vegetables; they are added to food to act as thickeners, gelators, emulsifiers, encapsulants and bulking agents. The selection of a specific polysaccharide for a food formulation, driven by a desired functionality, is inextricably linked to the polymer's physical properties and structure. Although most food polysaccharides are water dispersible, their behaviour is largely conditioned by the nature and extent of intermolecular associations. For instance, polysaccharide chains can be arranged into highly ordered crystalline structures, such as cellulose, which are insoluble in water and, at the other extreme, fluctuating, disordered coils, as in the case for some amorphous hemicelluloses.

Starch

Starch is one of the most abundant plant polysaccharides and is the main component in many raw and processed foods. While commonly considered to be a single ingredient, starch is, in fact, a blend of polysaccharides with varying molecular weight and branching, composed of linear amylose and branched amylopectin. Native starch is found in vegetal sources as water-insoluble semicrystalline granules that possess a complex hierarchical architecture characterised by at least four structural levels. Starch granules (ca. one to hundreds of μm) are composed of concentric semicrystalline and amorphous growth rings (ca. 120–400 nm) containing purported 'blocklet' structures with dimensions thought to represent the length of a single amylopectin chain. The semicrystalline rings are composed of lamellar stacks of alternating amorphous and crystalline regions (9–10 nm); the crystalline regions are thought to comprise mainly amylopectin side chains which are organised in double helices, whereas the amorphous regions are mainly linear amylose chains and less ordered amylopectin branch points. These helices are organised laterally into different crystalline unit cell structures, namely monoclinic (A-type), mainly found in cereal starches and related to short polysaccharide double helices, hexagonal (B-type) associated with long double helices found in tubers and high amylose starches and mixtures of A- and B-type, imaginatively known as C-type, commonly found in legumes. Blazek and Gilbert [35] have extensively reviewed starch characterisation with SAS.

The vast majority of published SAS studies have investigated the extent of lamellar organisation and associated changes due to amylose-to-amylopectin ratio, temperature and processing. The intensity of the lamellar peak (apparent at q ca. 0.07 A^{-1}) decreases with increasing amylose and increases with increasing moisture to the point where water is in excess. The former is consistent with decreased contrast between crystalline and amorphous regions due to localisation of amylose chains within different regions of the lamellae; the latter is consistent with a 'liquid crystalline' model which proposes that water acts as a plasticiser in which the amylopectin branch points, acting as flexible spacers, allow the polysaccharide double helices to be decoupled from the polymer backbone and aligned into lamellae. The combination of SAXS and SANS in the limit of low q has allowed larger-scale structures to be highlighted in dry and hydrated native starches; in the absence of water, growth ring substructures (blocklets) are apparent in SAXS, whereas, in the hydrated state, growth rings or larger blocklets are detected in SANS [36]. Recent works on native starches include [37,38].

The vast majority of starch consumed will have undergone some form of processing. This typically combines heat and humidity leading to starch gelatinisation with structural changes occurring at multiple levels including lamellar disruption and crystallite melting [39,40]. The influence of heat treatment at 10–30% moisture on subsequent starch digestion has been recently investigated [41]. Martinez-Sanz et al. [42] have explored the extent to which microalgae can be added to starch to limit water accessibility and to mitigate against gelatinisation. Beyond heating, starch is often subjected to other treatments to facilitate its processing or to adapt its properties to target requirements for specific food

products. For instance, ultrasonic treatment induces structural changes in the lamellae, promoting greater granule swelling without affecting the crystal structure. SAXS has been used recently to investigate structural changes arising from pulsed electric fields, shearing, grinding and chemical modification [43–47]; however, many of these studies merely describe changes to the scattering rather than embarking on full analysis. It is also clear that many studies suffer from restricted q range, typically not reaching sufficiently low q to reveal the full extent of hierarchical structural changes. As far as processing is concerned, it is noteworthy that measurements are also often limited to study before and after the process itself; however, significant, and largely unexploited, opportunities exist to monitor changes throughout a process in real time. For example, Doutch et al. [48] measured the loss in lamellar order and starch gel formation during an emulated stirring and cooking process using a rapid viscoanalyser modified for SANS measurements; in this case, the neutron beam was able to penetrate a sample container and impeller that were both constructed from aluminium yielding *in operando* information. Yang et al. [49] studied starch gelatinisation during high pressure processing in waxy (high amylopectin) starches using SAXS, monitoring lamellar peak intensity and width throughout the process.

From the perspective of nutrition, understanding the factors affecting starch digestibility is essential. After consuming starchy foods, enzymes in the small intestine are able to digest a fraction of the starch, converting it into glucose, whereas another fraction, known as resistant starch, is not digested, providing several health benefits via bacterial fermentation to produce short-chain fatty acids. The degree of starch gelatinisation is known to affect digestion rates and is conditioned by the extent and type of processing to which starch has been subjected during manufacture. It is also affected by the way in which food is prepared before its consumption; for example, the rapid heating rates provided by microwaves lead to lamellar disruption before the onset of gelatinisation, whereas refrigeration of cooked rice for

Figure 4

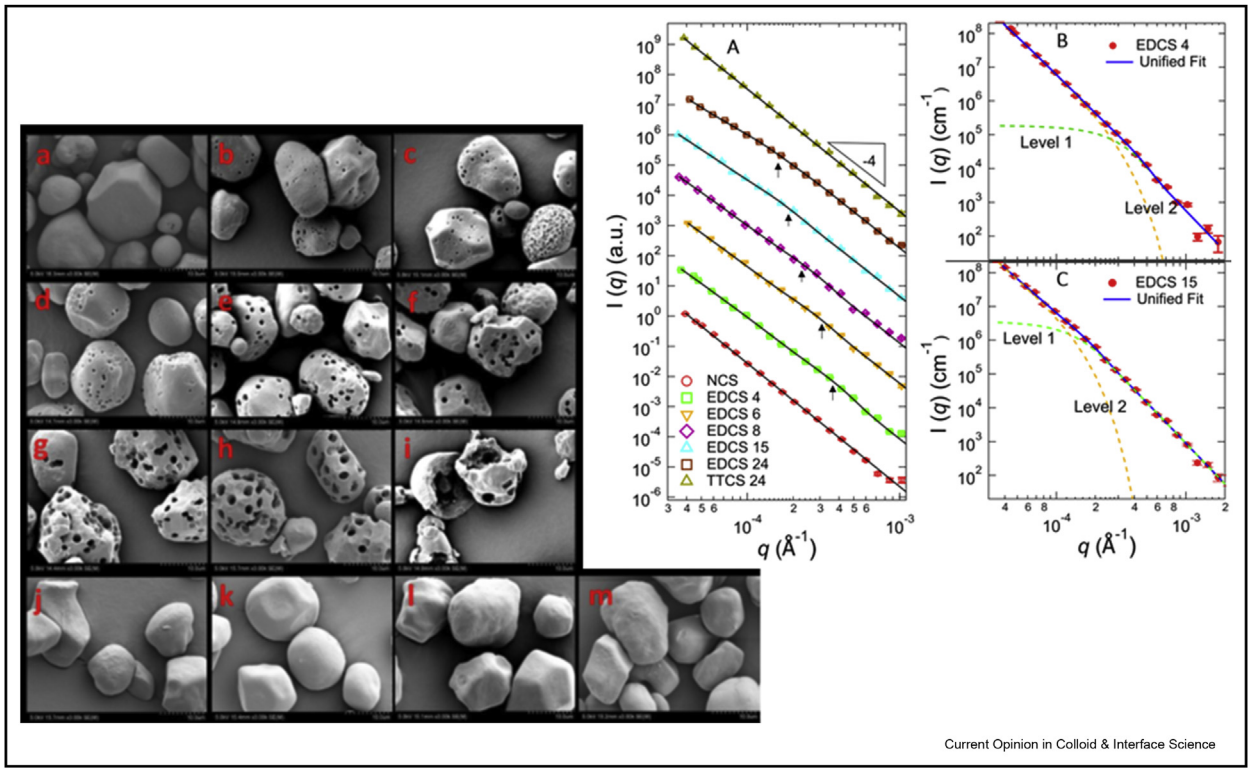

(Left) Scanning electron micrographs of normal corn starch residues hydrolysed by amyloglucosidase for 0 h **(a)**, 0.5 h **(b)**, 1 h **(c)**, 2 h **(d)**, 4 h **(e)**, 6 h **(f)**, 8 h **(g)**, 15 h **(h)** and 24 h **(i)** and thermally treated for 1 h **(j)**, 4 h **(k)**, 8 h **(l)** and 24 h **(m)**. Scale bar: 10 μm (Right) USANS analysis of native and porous corn starches **(A)** USANS profiles of native corn starch (NCS) and amyloglucosidase hydrolysed corn starches by 4, 6, 8, 15 and 24 h (enzymatically digested corn starch, EDCS). TTCS is thermally treated corn starch i.e. as EDCS but without enzyme. The scattering curves are vertically shifted for clarity. The power-law inflection points are indicated by the arrows **(B, C)** USANS profiles of corn starch residues hydrolysed for 4 h (B) and 15 h (C). The unified model fits are shown as a solid black line in each plot. The two fit levels are presented as dashed green (Level 1) and orange (Level 2). Reprinted from Carbohydrate Polymers 212, Zhi Yang, Xu Xu, Ravnit Singh, Liliana de Campo Elliot P. Gilbert, Zhonghua Wu, Yacine Hemar, Effect of amyloglucosidase hydrolysis on the multi-scale supramolecular structure of corn starch, 40–50, Copyright (2019), with permission from Elsevier [53]. USANS, ultra-small-angle neutron scattering.

12 h before consumption promotes the formation of resistant starch. The structural changes taking place during digestion have been investigated by SAS techniques in a relatively limited number of studies and on mostly unprocessed starches. For example, Blazek and Gilbert [50] investigated a range of native starches extracted from different sources and continuously monitored the change in SANS during enzymatic hydrolysis with amylose and amyloglucosidase. Chen et al. have investigated acid hydrolysis [51] and gastrointestinal digestion [52] of waxy, high and normal amylose starches with SAXS. Yang et al. [53] have recently used USANS and SANS to study amyloglucosidase hydrolysis in corn starch and compared pore dimensions formed during hydrolysis, extracted using unified models, to those measured using SEM; in addition to probing a large sample size and therefore granule population, USANS has the advantage of being able to provide information on surface and interior pores, the latter being inaccessible to SEM with large sampling size (Figure 4).

Cellulose and plant cell wall polysaccharides

Starch and cellulose are both polysaccharides but differ in terms of the bonds between monomer units; cellulose is a linear homopolysaccharide of D-glucose units connected by (1,4)-β-glucosidic bonds in contrast to amylose with (1,4)-α-glucosidic bonds (and amylopectin possessing (1,6)-α-glucosidic branches). Cellulose is the major component of plant cell walls (PCWs); the latter are composite materials in which semicrystalline cellulose is embedded in an amorphous multicomponent matrix, composed of other polysaccharides, of which hemicelluloses and pectins are the most abundant. While cellulose microfibrils represent the main building block in most PCWs, the specific properties of each plant tissue are strongly determined by the matrix cell wall composition and the interactions established between the different cell wall constituents. Understanding the structural role of such constituents is relevant to the food industry to optimise extraction methods to isolate polysaccharides from PCWs as individual food ingredients, the use of PCW fractions as food additives with specific rheological or textural properties and to understand the possible nutritional benefits of plant-based foods based on composition and bioavailability. Human alimentary enzymes are not able to digest cellulose, but this nondigestible constituent of insoluble dietary fibre can act as a prebiotic for gut bacteria and enhancement of gut health.

When cultivated in a saccharide−rich medium, the bacterium *Gluconoacetobacter xylinus* forms hydrogels of cellulose (pellicles) that can be used as cell wall analogues, permitting studies into the specific effect of different PCW components through incorporation into the synthesis medium. Martínez-Sanz et al. have both reviewed the application of SAS to PCWs [54] and have performed SAS and USANS on a variety of pure and composite hydrogels systems with and without selectively deuterated cellulose [55−58]. Owing to differential solvent accessibility, SANS and SAXS provide complementary information. They identified distinct interaction mechanisms of cellulose with matrix PCW polysaccharides including arabinoxylan, xyloglucan, mixed-linkage glucan and pectin. In the case of pectin [59−61], SAS techniques were combined with rheological characterisation, showing that two different fractions of pectin exist in PCWs. The impact of hydrothermal, mechanical and drying treatments, as representative food processing methods, on cellulose binding capacity for food polyphenols has also been assessed [62]. Although the conclusions drawn from cited works are based on model cellulose hydrogels, the same approach has been successfully applied to characterise the structure of PCW extracted from onion, carrot and apple (unpublished results).

Other carbohydrates

Alginate, an anionic polysaccharide, is the most abundant marine biopolymer and occurs in the intercellular mucilage and algal cells of brown seaweeds in the form of calcium, sodium and magnesium salts of alginic acid. Schuster et al. [63] considered the potential of alginate gels, in which parallel capillary channels had been formed through controlled calcium ion diffusion, to act as scaffolds for aligned skeletal muscle cell growth for cultured meat; Yu et al. [64] investigated the rheological and structural properties of two gel-forming arabinoxylan fractions isolated from *Plantago ovata* seed mucilage under nongelled conditions using SAS. Despite similar molecular dimensions and chain rigidity, the two polymers were found to display dramatically different rheological behaviour thought to be related to variations in the carbohydrate sequence of the side chains. Curdlan is a water-insoluble microbial polysaccharide which is insoluble in water but soluble in alkaline solutions. It is used in the food industry as a stabiliser, but fibrillar gels formed either by heating aqueous suspensions or neutralising alkaline solutions may also function as encapsulants. Maki et al. [65] used SAXS to investigate the structural variation and fibril orientation within gels formed when $CaCl_2$ was allowed to diffuse into a curdlan solution. Konjak glucomannan is a soluble dietary fibre with high water-holding capacity. Lopez-Rubio et al. [66] investigated its interaction with low- or high-molecular-weight chitosan—a pH-sensitive polysaccharide obtained from the hard outer skeleton of shellfish and cell walls of fungi. The resultant system generates an interpenetrating hydrocolloid network with the potential to produce an appetite suppressing ingredient able to swell under gastric pH conditions.

Maturation provides whisky with a mild and smooth texture by removing irritating alcoholic flavours.

Combining SAXS and DLS, Morishima et al. [67] explored the structure of whisky as a function of maturation time from 'new-make' to 25 years with the intent of correlating changes to sensory response, specifically 'smoothness'. They show that two scattering components are present corresponding to the clusters formed by extractives from oak casks during maturation, which are not present in the freshly distilled whisky. Furthermore, only small clusters increase in concentration during maturation, whereas the large cluster component is independent of maturation time. Although not specifically stated, it is likely that these small clusters are largely composed of small carbohydrate molecules. They propose that the small cluster component is crucial for obtaining flavour, whereas the large cluster component is associated with alcoholic irritation of the whiskies.

Proteins

The greater diversity of amino acid moieties and combinations thereof, over monosaccharides, and differences in their responses to external effects such as pH and temperature, make food proteins significantly more complex than polysaccharides. Apart from contributing to the nutritional quality of food, proteins act as integral components to food formulations to provide a range of functionalities including as emulsifiers, gelators and encapsulants, and edible packaging and films.

Plant proteins

The storage proteins in wheat are collectively referred to as gluten, although gluten is actually an aggregate of two families of proteins: gliadins and glutenins, soluble and insoluble in ethanol, respectively. Urade et al. [68] have reviewed progress on the characterisation of gliadins with SAXS. Interestingly, the authors highlight the formation of hierarchical nanoscale structures with internal density fluctuations at high protein concentrations whose separation decreases with the addition of salt; the latter is relevant to bread because salt is used to tighten dough behaviour. Soy protein isolate is widely used in meat, beverage and nutraceutical products for nutritional reasons, as well as having applications in water absorption, thickening, gelling, emulsifying and foaming. The two major components of soy protein isolate are glycinin (a hexameric globulin consisting of acidic and basic subunits) and β-conglycinin (a trimeric glycoprotein). Xiao et al. [69] have investigated the behaviour of both proteins under heat treatment in acidic or alkaline environments. Acidic conditions result in hydrolysis to polypeptides. P(r) functions from SAXS reveal a globular structure for the monomers of β-conglycinin which partially unfold on heating; in contrast, glycinin exhibits unfolding in the absence of heat and that increases with heating. In alkaline conditions, no hydrolysis occurs and globular structures are retained in both proteins; aggregation occurs on heating but more readily so in glycinin. Lysine is one of the most limiting essential amino acids in wheat and strategies to increase the nutritional value and production of bread wheat are of major significance in agricultural science. Dihydrodipicolinate synthase (DHDPS) catalyses the first step in the lysine biosynthesis pathway of plants. As an alternative to the seven step process for isolating DHDPS, Gupta et al. [70] used SAXS to determine the structure of recombinant DHDPS from bread wheat *Triticum aestivum* using SAXS. Rasheed et al. [71] used SAXS to assess the structure of an unknown 27 kDa protein isolated from the ginger rhizome. Sun et al. [72] have investigated denaturation and complex formation between α-lactalbumin and sodium dodecyl sulphate—a generally recognised as safe ingredient for food use—with SAXS, complemented with isothermal titration calorimetry and circular dichroism as a function of concentration and ratio, interpreting the scattering with a 'beads-on-a-string' model.

Dairy proteins

The composition of milk varies with animal with bovine milk being the most commonly studied. The proteins fall into two broad categories, caseins and whey proteins. The principal whey proteins are α-lactalbumin and β-lactoglobulin, although an array of other proteins including lactoferrin, serum albumin, lysozyme and immunoglobulins are also present with composition depending on the stage of the lactation cycle and health of the animal. The vast majority of SAS studies have focussed on the structure of casein micelles which are self-assembled colloidal structures comprising four casein proteins (α_{S1}-, α_{S2}-, β- and κ- at an approximate ratio of 4:1:4:1) and minerals in the form of colloidal calcium phosphate (CCP) nanoclusters. Average micelle sizes range from 50 nm to 230 nm in diameter for individual cows and vary across a lactation cycle. It is generally accepted that the surface of the micelle is largely covered by a brush layer of κ-casein. However, until relatively recently, there has been considerable debate concerning the internal structure and assembly of casein proteins in the micelle with contrast variation SANS (to separate protein and CCP contributions) and SAXS having been actively exploited. SAS has been described either using the submicelle model or the nanocluster model, the common feature between the models being the recognition of CCP as an integral part of the micelle internal structure. The submicelle model describes casein micelles as small protein micelles (submicelles) linked together by bridging CCP whereas the nanocluster model considers CCP nanoparticles to be randomly distributed within the micelle and having protein molecules surrounding them. de Kruif et al. [73] have provided an authoritative summary of SAS dealing with this topic. The nanocluster model has now been accepted with evidence most recently coming from measuring SAXS around the calcium L_2/L_3 absorption edges with RSoXS [74,75].

Scattering curves can be described by a hierarchical structural model with features corresponding to (a) overall micelle size, (b) large heterogeneous regions of 'incompressible' protein and water channels, (c) CCP clusters and (d) dense protein overlap regions [75] as shown in Figure 5. The CCP structure factor peak observed in RSoXS at q = 0.032 $Å^{-1}$ is not explicitly observed in SAXS unless in dried powders [76] but is observed in contrast variation SANS [73]. In the casein micelle, rather than representing a characteristic separation due to a repulsive interaction, it rather describes an exclusion zone around each CCP particle, which is bound to phosphoserine sites on the α- and β-casein proteins, of which, there are a limited number; the α-caseins and β-caseins also bind through hydrophobic interactions. RSoXS, together with ASAXS, has been used to study the casein micelles in iron-fortified milk, indicating that iron is co-located within the CCP nanoclusters [77].

While bovine milk has been the most intensively investigated, Ingham et al. [78] used conventional and resonant SAXS to investigate structural differences of casein micelles compared to goat and sheep milk. The correlation length between, and size of, CCP nanoparticles, was the same, although larger scale structures—including 'incompressible regions', water channels and the overall size of the casein micelle itself—had different sizes and relative scattering intensities which they speculate are associated with differences in protein composition and hydration. Similarly, Day et al. [79] used SAXS to study casein micelles from individual cows to investigate whether genetic variants of β- and κ-casein alter the internal structure. However, despite the large natural variation in micelle size and protein genetic variants, all samples have identical scattering patterns in the intermediate and high q region, implying that the internal structures of casein micelles are the same regardless of micellar size or protein genetic variation.

The structure evolution of casein micelles under high hydrostatic pressure up to ca. 1000 MPa was investigated *in situ* using synchrotron SAXS at room temperature [80]. A decrease in scattering during treatment suggested the disruption of both casein micelles and CCP nanoclusters. A scattering peak around 0.02 $Å^{-1}$ appears which increases with pressure that the authors ascribe to "submicelles". Data were not fitted formally but rather described using a linear combination of the low and high pressure scattering patterns. Pressure results in irreversible changes to the scattering.

Calcium chelators, including citrates and phosphates, are often added to milk to improve the heat stability of milk products, whereas ethylenediamine tetraacetic acid (EDTA), another chelator, is added to milk to improve its foaming properties. These effects are achieved by inducing a shift in the protein-mineral equilibrium between casein micelles and milk serum, resulting in micelle dissociation. Transglutaminase (TG) treatment has been shown to prevent or reduce the extent of dissociation of casein micelles. Lam et al. [81] measured the SAXS from both TG-untreated and TG-treated casein micelles to which EDTA had been added to assess the extent of TG-mediated protection.

The structure, dynamic size and stability of casein micelles play important roles in the processing of milk and its conversion to various dairy products such as cheese, yoghurt and milk protein powder concentrates. Cheese is obtained by first coagulating milk; this is often achieved using the clotting enzyme rennet which has high specificity to cleave Phe105-Met106 in κ-casein. Owing to restrictions of its use for religious and vegetarian dietary reasons, animal rennet has been increasingly replaced by bacterial rennet. Increasing cheese consumption has also driven the search for rennet substitutes such as plant-based proteases (e.g. extracted from kiwi fruit, melon and ginger) which may also have broader proteolytic activity to α- and β-caseins and accordingly result in gels with different firmness. Li et al. [82] compared the behaviour of two enzymes used to initiate milk coagulation, namely rennet, and a serine protease from tamarillo referred to as 'tamarillin'. USANS showed that there are no differences in the large-scale structures of either casein gel with two power law regions associated with mass fractal and Porod scattering with a crossover point at q ca. 0.003 $Å^{-1}$, a dimension corresponding to a typical size for casein micelles; however, SAXS reveals differences in fine structure with peaks associated with the separation of CCP nanoclusters occurring at lower q in the tamarillin gels consistent with less dense structures.

Figure 5

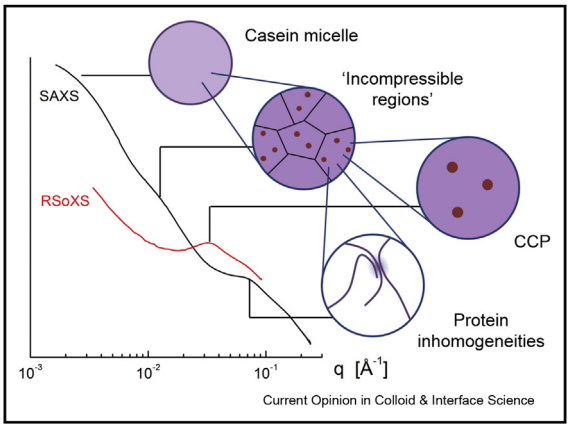

Comparison of SAXS and calcium-edge resonant soft SAXS from casein micelles demonstrating its complex hierarchical structure. Figure courtesy of Bridget Ingham. CCP, colloidal calcium phosphate; RSoXS, resonant soft X-ray scattering; SAXS, small-angle X-ray scattering.

Relevant to sodium reduction in cheese, Kuo et al. [83] investigated heat-induced gels of emulsions of whey protein isolate and anhydrous milk fat with varying protein, fat and NaCl content as well as homogenisation pressure. The radii of gyration of protein aggregates and fat globules were extracted from SAXS, and they demonstrate that fat globule size is a better indicator for sodium release that emulsion radius. Sodium caseinate, produced from milk after removal of calcium, phosphate, lactose, fat and whey proteins, is widely used in food manufacturing as an emulsion stabiliser and foaming agent. Using SAXS, as well as turbidity and DLS, Smialowska et al. [84] investigated the effect of calcium on the aggregation behaviour of caseinates and showed that below a critical concentration, mainly small protein clusters are present, whereas above the aggregation point, larger aggregates containing incompressible regions are formed. Aggregation of sodium caseinate is affected by the presence in the aqueous phase of disaccharides; Huck-Iriart et al. [85] have studied the influence of sucrose on the stability of sodium caseinate–stabilised sunflower O/W emulsions, while Oca-Ávalos et al. [86] have investigated the same system during gelation with glucono-δ-lactone as a means of forming emulsion-based gels for structuring food. Food structuring can also be achieved with protein fibrils and the use of whey proteins, such as β-lactoglobulin, for fibril formation is a particularly attractive approach due to low cost and availability. While whey protein fibrils are commonly produced at acidic pH, SAXS has recently been used to investigate stability at pH values more relevant for food application [87]. Characteristic q^{-1} scattering associated with fibril formation is observed, but close to the isoelectric point for the protein, aggregate formation is apparent with dramatic increases in low q scattering.

Animal proteins

There has been recent activity in the use of SAXS to describe meat quality, a generic term that describes properties and perception including tenderness, juiciness and flavour. SAXS diffraction peaks yield information on myofibril muscle and intramuscular fat structure. In a study of lamb and sheep meat, Hoban et al. [88] used SAXS to provide insight on actin, myosin and collagen fibrils and the extent to which they may be correlated with various attributes of meat quality. For example, measured fat content determined using conventional techniques could be correlated with the intensity of an isotropic scattering ring at 0.145 A^{-1}. As another attribute of quality, colour is essential to consumer acceptability with dark meat muscle colour being less attractive to consumers. Taking beef longissimus thoracis muscles, divided into 'light', 'medium' and 'dark' colour groups, and monitoring changes in the equatorial peaks in the small-angle region, Hughes et al. [89] showed that dark muscles had longer myosin–myosin and myosin–actin myofilament lattice spacings; in addition, the intensity ratio between the peaks at ca. 0.015 and 0.030 A^{-1} (associated with myosin filaments and myosin and actin filaments, respectively) is lower in dark versus light or medium colour samples. They propose that the change in transverse spacing of muscle fibres that occurs with the pH decline post-mortem is critical to light scattering development. In the rigor state, myosin and actin filaments are "locked" by actomyosin bonds with the result that the size of the myosin head region will influence the interfilamental space with myosin able to expel water from the sarcomere to the extracellular space. Liu et al. [90] compared relaxed and rigor states in porcine meat through comparison of the relative intensities of same equatorial peaks and provide recommendations on pH and temperature to avoid the onset of rigor.

Gelatin is widely used to provide elasticity, viscosity, and structural stability in foods and is obtained by breaking the triple-helix structure of collagen into single-stranded molecules. Physical gels of gelatin are formed when a temperature decrease transforms random coils into partially renatured ordered triple helices; the networks formed are held together by hydrogen-bonded junction zones but, at physiological temperatures and above, gels reversibly melt into a solution. To stabilise gelatin gels, chemical or enzymatic cross-linking agents can be used, for example, glutaraldehyde. As a precursor to rheo-SANS studies, Yang et al. [91] investigated differences in the hierarchical structure of physical and chemically cross-linked gels formed in a Couette cell. A relatively homogeneous network is formed in the physical gels, whereas in chemically cross-linked gels, small cross-linked aggregates are formed; these structural variations can be related to differences in behaviour under large and small deformation conditions.

Protein–polysaccharide systems

Under certain conditions, oppositely charged proteins and polysaccharides interact with each other to yield a dense fluid (complex coacervate) in equilibrium with a dilute phase. Different from individual protein or polysaccharide systems, coacervates exhibit well-organised supramolecular structures with a wide range of food-relevant functionalities. Xu et al. [92] studied the interaction of β-lactoglobulin A (βLgA) with oligogalacturonic acids (OGAs) of varying number of sugar residues. They found that (anionic) OGAs require a minimum length of 7 or 8 sugar residues to interact with (cationic) βLgA. SAS showed that when OGAs were in excess, βLgA molecules were stabilised upon OGA binding and no subsequent aggregation was observed. However, when βLgA was present in excess, the solution became turbid and large mass-fractal aggregates of primary particles are formed which assemble from βLgA/

OGA complexes; these multiscale structures eventually phase separate into two liquid phases. They also studied the interaction between the same protein and pectins with varying charged residues, the latter arising from different degrees and location of methyl esterification [93]. In the absence of the protein, pectins display scattering characteristic of a flexible chain with finite persistence length. At equimolar ratio, with increasing q, three regions are observed associated with mass fractal, rough surface fractal and Gaussian polymer behaviour. With increasing protein-to-pectin ratio, the crossover between mass and surface fractal scattering shifts to lower q. An enhanced understanding of the system was obtained using deuterated protein and solvent contrast variation SANS to decouple the contributions from the two components. Electrosprayed chitosan–gelatin networks have been investigated as food-grade delivery vehicles for anthocyanin [94]. Clusters are formed because of the electrostatic interactions between the positively charged amino groups in chitosan and negatively charged amino acid residues in gelatin; scattering is interpreted using a two-level unified model.

Tea polyphenols exhibit strong binding affinity with proteins, and such interactions have been proposed to contribute to a range of health-promoting outcomes including neuroprotection against Parkinson's disease. Shi et al. [95] investigated the change in conformation and aggregation behaviour during complexation of four systems containing one of two model proteins—bovine serum albumin (BSA) and trypsin—and one of two tea polyphenols: catechin and epigallocatechin gallate (EGCG). Using SAXS, complemented with fluorescence spectroscopy, they found that trypsin exhibits partial unfolding in the presence of EGCG and catechin, with unfolding increasing with increasing tea polyphenols. BSA has a relatively higher resistance to unfolding, with the presence of tea polyphenols helping to preserve its protein conformation. The additional gallic acid group in EGCG has significantly stronger capability than catechin to interact with trypsin and BSA to induce aggregation. They find that the aggregates bridged by EGCG are densely packed with a relatively smooth surface, and the synergistic unfolding of trypsin enhances binding and aggregation.

Nonedible applications

With enhanced awareness of waste generation and deriving value from waste streams in food processing, there is elevated research activity in the use bio-based materials for food packaging. Differences in low q SAXS behaviour in starch films loaded with lignocellulose via melt mixing and extrusion have been proposed to correlate with reduced water permeability [96]. Other carbohydrate-based packaging systems investigated include chitosan–cellulose nanocrystals [97] and corn starch films containing microalgae [42,98]. Proteins are also being investigated as sources for biodegradable packaging; for example, Romani et al. [99] have investigated films formed from thermal- and pH-induced gels of mixed muscle proteins extracted from Whitemouth croaker.

An interesting and emerging application is the use of SAS for the study of nanotoxicology and food safety. Oral ingestion is an important uptake route for aluminium and may arise from food additives, packaging and kitchenware; correlations have been proposed between the use of aluminium-containing products and Alzheimer's disease and breast cancer. Sieg et al. [100] have explored the fate of aluminium nanoparticles, in the form of soluble ionic aluminium ($AlCl_3$), elementary metallic aluminium (Al^0) and mineral oxidised aluminium (Al_2O_3); the three species were studied separately in a complex artificial digestion system of three steps: saliva, gastric juice and intestinal juice. SAXS was used to extract details of the nanoparticle size distribution and agglomeration; combined with an arsenal of other techniques, including ion beam microscopy and ion mass spectroscopy, they found that metallic and oxidised aluminium particles are almost unaffected in saliva, agglomerate in gastric juice and release ions into the fluid. In the intestine, these agglomerates tend to deagglomerate into primary particles, whereas free ions form solid complexes that can differ significantly from primary particles in their size, shape and density. They find that particles and dissolved ions can be transformed into one other with surface element composition changing; they conclude that orally ingested nanoparticles probably reach the intestinal epithelium. In a related study, the aggregation of nanoparticles of silver—an antimicrobial agent—under the same conditions and in the presence of oil, starch, skimmed milk powder and mixtures thereof was investigated [101]. E234, also known as nicin, is a food additive approved by the European Union as an antifungal preservative. As a means of improving delivery, Chatzidaki et al. [102] have explored using reverse micelles as a nisin carrier. Antimicrobial activity was investigated with micelles against *Staphylococcus aureus* on lettuce leaves and *Listeria monocytogenes* in minced meat; SAXS was used to determine particle size of the micelles in olive oil or sunflower oil; however, interpretation is complicated by the presence of peaks intrinsic to the pure solvents.

Conclusions

In this review, I have deliberately sought to provide sufficient description of the food systems as well as the purpose of their study, alongside the basis for data analysis, to provide useful information for the small-angle scattering expert who is interested in learning more about how this method has been applied to food colloids and the food specialist that wishes to gain

knowledge of the former. As colloid scientists, we are aware that the 'interface' is critically important; this is no less so when one acknowledges the great opportunities for new findings that exist at the 'interface' of established methods.

While the increase in the uptake of SAS methods is encouraging, the extent to which they are being exploited and the difference between what can be extracted from the data compared to what should be varies enormously; unfortunately, this includes underinterpretation, overinterpretation and no interpretation whatsoever. Indeed, as is the case in many scientific fields, there are some concerning examples published in the literature where data interpretation is incorrect and it is certainly evident that some of the systems reported could be investigated more 'robustly'. The rise in the number of institutes taking delivery of state-of-the-art laboratory-based SAXS equipment, but perhaps without the necessary background in the technique, may add to the problem where ease of use outweighs rigorous analysis. This is very much in contrast to the major issue faced in the neutron field where access to instrumentation becomes a dominant consideration [103]. My personal view is that it is incumbent upon the scattering 'experts' to assist, to ensure that the field continues to progress and to showcase the wealth of information that can be extracted when these methods are correctly exploited.

An attempt to prepare a review that highlights the latest activities in food colloids with small-angle scattering methods has not been a small undertaking, and it is hoped that this work will initiate interest from both food and SAS communities alike and decrease the dialogue barrier so that new knowledge of food materials, to which we all have personal experience on a daily basis, can be generated.

Funding

This research did not receive any specific grant from funding agencies in the public, commercial or not-for-profit sectors.

Conflict of interest

Nothing declared.

Acknowledgements

The author would like to thank Karl Mutimer for design of the graphical abstract, Amparo Lopez-Rubio and Marta Martinez-Sanz for highlighting recent activities from the Food Safety and Preservation Department at IATA (CSIC) on protein-polysaccharide systems and food packaging, Andrew Clulow and Adrian Hawley who brought to my attention some recent outputs from the Australian Synchrotron and Kumudika de Silva who provided clarity on cholesterol control mechanisms in humans. The author would also like to ackowledge all members (past and present) of the food materials science group at ANSTO, as well as collaborators from around the world, for their contributions to this rich field of science.

References

Papers of particular interest, published within the period of review, have been highlighted as:

* of special interest
** of outstanding interest

1. Aguilera JM, Lillford PJ: **Structure–property relationships in foods**. In *Food materials science: principles and practice*. Edited by Aguilera JM, Lillford PJ, New York: Springer; 2008:229–253.

2. ** Vilgis TA: **Soft matter food physics—the physics of food and cooking**. *Rep Prog Phys* 2015, **78**:124602, https://doi.org/10.1088/0034-4885/78/12/124602.
Vilgis explores in exquisite detail the physics of food and cooking including some experiments that can be attempted in the kitchen.

3. ** SAS Portal. http://smallangle.org/content/Resources.
Assembled by the canSAS group, this is a valuable resource for both novice and expert small-angle scatterers, providing comprehensive links to tutorials, software, books and journal articles.

4. ** Hammouda B: *The SANS toolbox*. 2008. www.ncnr.nist.gov/staff/hammouda/the_SANS_toolbox.pdf.
An excellent freely available resource on all aspects of small-angle neutron scattering including instrumentation.

5. * Lopez-Rubio A, Gilbert EP: **Neutron scattering : a natural tool for food science and technology research**. *Trends Food Sci Technol* 2009, **20**:491–500, https://doi.org/10.1016/j.tifs.2009.07.008.
Now ten years old, this paper highlights not only the use of SANS, but neutron techniques more broadly, in food materials science.

6. ** Ramel PR, Co ED, Acevedo NC, Marangoni AG: **Structure and functionality of nanostructured triacylglycerol crystal networks**. *Prog Lipid Res* 2016, **64**:231–242, https://doi.org/10.1016/j.plipres.2016.09.004.
Extensive review of fat crystallisation on the nano- to micron length scales including polymorphism.

7. * Pink DA, Townsend B, Peyronel F, Co ED, Marangoni AG: **Sheared edible oils studied using dissipative particle dynamics and ultra small angle X-ray scattering: TAGwood orientation aggregation and disaggregation**. *Food Funct* 2017, https://doi.org/10.1039/c7fo00514h.
This work employs both USAXS and mesoscopic computational fluid simulations to investigate TAG nanoplatelet aggregation under variable shear conditions.

8. Townsend B, Peyronel F, Callaghan-Patrachar N, Quinn B, Marangoni AG, P DA: **Shear-induced aggregation or disaggregation in edible oils : models, computer simulation, and USAXS measurements**. *J Appl Phys* 2017, **122**:224304, https://doi.org/10.1063/1.5004023.

9. Nikolaeva T, Adel R Den, Velichko E, *et al.*: **Networks of micronized fat crystals grown under static conditions**. *Food Funct* 2018, **9**:2102–2111, https://doi.org/10.1039/c8fo00148k.

10. * Miyagawa Y, Shintani K, Katsuki K, Nakagawa K, Adachi S: **Thermal and structural changes of rapeseed oil during isothermal storage at low temperature**. *Food Struct* 2017, **11**:8–15, https://doi.org/10.1016/j.foostr.2016.12.004.
A carefully-performed multi-technique evaluation of oil crystallisation relevant to chilled food including time-resolved SAXS during isothermal storage.

11. Lambert A, Bougrioua F, Abbas O, *et al.*: **Temperature dependent Raman and X-ray diffraction studies of anhydrous milk fat**. *Food Chem* 2018, **267**(ptember 2017):187–195, https://doi.org/10.1016/j.foodchem.2017.09.006.

12. Ramel PRR, Peyronel F, Marangoni AG: **Characterization of the nanoscale structure of milk fat**. *Food Chem* 2016, **203**:224–230, https://doi.org/10.1016/j.foodchem.2016.02.064.

13. Zychowski LM, Logan A, Augustin MA, *et al.*: **Effect of phytosterols on the crystallization behavior of oil-in-water milk fat emulsions**. *J Agric Food Chem* 2016, **64**:6546–6554, https://doi.org/10.1021/acs.jafc.6b01722.

14. Truong T, Janin S, Li BZ, Bhandari B: **Effect of crystalline structure on oxidation of fish oil in stearin:fish oil mixtures**.

Food Bioprocess Technol 2016, **9**:792–800, https://doi.org/10.1007/s11947-015-1664-z.

15. * Lopez C, Cheng K, Perez J: **Thermotropic phase behavior of milk sphingomyelin and role of cholesterol in the formation of the liquid ordered phase examined using SR-XRD and DSC**. *Chem Phys Lipids* 2018, **215**(May):46–55, https://doi.org/10.1016/j.chemphyslip.2018.07.008.
Elegant study coupling SAXS and XRD with DSC highlighting the influence of cholesterol on the phase behaviour of sphingomyelin.

16. Chiappisi L, Grillo I: **Looking into Limoncello: the structure of the Italian liquor revealed by small-angle neutron scattering**. *ACS Omega* 2018, https://doi.org/10.1021/acsomega.8b01858.

17. Sagalowicz L, Moccand C, Davidek T, *et al.*: **Lipid self-assembled structures for reactivity control in food**. *Phil Trans A* 2016, **374**:20150136.

18. Shao X, Bor G, Al-hosayni S, Salentinig S: **Structural characterization of self-assemblies of new omega-3 lipids: docosahexaenoic acid and docosapentaenoic acid monoglycerides**. *Phys Chem Chem Phys* 2018, https://doi.org/10.1039/c8cp04256j. 10.1039/c8cp04256j.

19. Yaghmur A, Al-hosayni S, Amenitsch H, Salentinig S: **Structural investigation of bulk and dispersed inverse lyotropic hexagonal liquid crystalline phases of eicosapentaenoic acid monoglyceride**. *Langmuir* 2017, **33**:14045–14057, https://doi.org/10.1021/acs.langmuir.7b03078.

20. Khaliqi K, Ghazal A, Azmi IDM, Amenitsch H, Mortensen K: **Direct monitoring of lipid transfer on exposure of citrem nanoparticles to an ethanol solution containing soybean phospholipids by combining**. *Analyst* 2017, **142**:3118–3126, https://doi.org/10.1039/c7an00860k.

21. Wei L, Li X, Guo F, Liu X, Wang Z: **Structural properties, in vitro release and radical scavenging activity of lecithin based curcumin-encapsulated inverse hexagonal (HII) liquid crystals**. *Colloids Surf, A* 2018, **539**(November 2017):124–131, https://doi.org/10.1016/j.colsurfa.2017.11.071.

22. Fonseca-Santos B, Satake CY, Calixto GMF, Dos Ssantos AM, Chorilli M: **Trans-resveratrol-loaded nonionic lamellar liquid-crystalline systems: structural, rheological, mechanical, textural, and bioadhesive characterization and evaluation of in vivo anti-inflammatory activity**. *Int J Nanomed* 2017, **12**:6883–6893, https://doi.org/10.2147/IJN.S138629.

23. ** Clulow AJ, Parrow A, Hawley A, *et al.*: **Characterization of solubilizing nanoaggregates present in different versions of simulated intestinal fluid**. *J Phys Chem B* 2017, **121**:10869–10881, https://doi.org/10.1021/acs.jpcb.7b08622.
Using SAXS, cryo-TEM, DLS and coarse-grained MD simulations, this study highlights differences in structure between the use of either DOPC or lecithin with sodium taurodeoxycholate to simulate intestinal fluid and the importance of standardised methods to reproduce more physiologically relevant conditons to assess nutrient solubilty.

24. Rezhdo O, Di Maio S, Le P, Littrell KC, Carrier RL, Chen SH: **Characterization of colloidal structures during intestinal lipolysis using small-angle neutron scattering**. *J Colloid Interface Sci* 2017, https://doi.org/10.1016/j.jcis.2017.03.109.

25. Boyd BJ, Salim M, Clulow AJ, Ramirez G, Pham AC, Hawley A: **The impact of digestion is essential to the understanding of milk as a drug delivery system for poorly water soluble drugs**. *J Control Release* 2018, **292**(August):13–17, https://doi.org/10.1016/j.jconrel.2018.10.027.

26. Binte Abu Bakar SY, Salim M, Clulow AJ, Hawley A, Boyd BJ: **Revisiting dispersible milk-drug tablets as a solid lipid formulation in the context of digestion**. *Int J Pharm* 2019, **554**(August 2018):179–189, https://doi.org/10.1016/j.ijpharm.2018.10.069.

27. * Clulow AJ, Salim M, Hawley A, Boyd BJ: **A closer look at the behaviour of milk lipids during digestion**. *Chem Phys Lipids* 2018, https://doi.org/10.1016/j.chemphyslip.2017.10.009.
Despite initial structural differences due to varied industrially-relevant processing conditions, lipid digestion of bovine milk results in the same final products albeit with different kinetics.

28. Salentinig S, Amenitsch H, Yaghmur A: **In situ monitoring of nanostructure formation during the digestion of mayonnaise**. *ACS Omega* 2017, **2**:1441–1446, https://doi.org/10.1021/acsomega.7b00153.

29. Cerqueira MA, Fasolin LH, Picone CSF, Pastrana LM, Cunha RL, Vicente AA: **Structural and mechanical properties of organogels : role of oil and gelator molecular structure**. *Food Res Int* 2017, **96**:161–170, https://doi.org/10.1016/j.foodres.2017.03.021.

30. Fasolin LH, Cerqueira MA, Pastrana LM, Vicente AA, Cunha RL: **Thermodynamic , rheological and structural properties of edible oils structured with LMOGs : influence of gelator and oil phase**. *Food Struct* 2018, **16**(January):50–58, https://doi.org/10.1016/j.foostr.2018.03.003.

31. Martins AJ, Cerqueira MA, Fasolin LH, Cunha RL, Vicente AA: **Beeswax organogels : influence of gelator concentration and oil type in the gelation process**. *Food Res Int* 2016, **84**:170–179, https://doi.org/10.1016/j.foodres.2016.03.035.

32. Martins AJ, Cerqueira MA, Cunha RL: **Fortified beeswax oleogels: effect of β-carotene on the gel structure and oxidative stability**. *Food Funct* 2017:4241–4250, https://doi.org/10.1039/c7fo00953d.

33. Okuro PK, Malfatti-gasperini AA, Vicente AA, Cunha RL: **Lecithin and phytosterols-based mixtures as hybrid structuring agents in different organic phases**. *Food Res Int* 2018, **111**(March):168–177, https://doi.org/10.1016/j.foodres.2018.05.022.

34. Zielbauer BI, Jackson AJ, Maurer S, *et al.*: **Soybean oleosomes studied by small angle neutron scattering (SANS)**. *J Colloid Interface Sci* 2018, **529**:197–204, https://doi.org/10.1016/j.jcis.2018.05.080.

35. * Blazek J, Gilbert EP: **Application of small-angle X-ray and neutron scattering techniques to the characterisation of starch structure : a review**. *Carbohydr Polym* 2011, **85**:281–293, https://doi.org/10.1016/j.carbpol.2011.02.041.
Detailed review on SAS as applied to starch including native materials, processing, gelatinisation and digestion.

36. Doutch J, Gilbert EP: **Characterisation of large scale structures in starch granules via small-angle neutron and X-ray scattering**. *Carbohydr Polym* 2013, **91**:444–451, https://doi.org/10.1016/j.carbpol.2012.08.002.

37. Li Z, Kong X, Zhou X, Zhong K: **Thermal properties of Indica rice starch with different amylose contents**. *RSC Adv* 2016:107491–107497, https://doi.org/10.1039/c6ra17922c.

38. Liu J, Wang X, Wen F, *et al.*: **Morphology, structural and physicochemical properties of starch from the root of Cynanchum auriculatum Royle ex Wight**. *Int J Biol Macromol* 2016, **93**:107–116, https://doi.org/10.1016/j.ijbiomac.2016.08.063.

39. Wang S, Zhang X, Wang S, Copeland L: **Changes of multi-scale structure during mimicked DSC heating reveal the nature of starch gelatinization**. *Sci Rep* 2016;(March):1–9, https://doi.org/10.1038/srep28271.

40. Kuang Q, Xu J, Liang Y, *et al.*: **Lamellar structure change of waxy corn starch during gelatinization by time-resolved synchrotron SAXS**. *Food Hydrocolloids* 2017, **62**:43–48, https://doi.org/10.1016/j.foodhyd.2016.07.024.

41. Wang H, Liu Y, Chen L, Li X, Wang J, Xie F: **Insights into the multi-scale structure and digestibility of heat-moisture treated rice starch**. *Food Chem* 2018, **242**:323–329, https://doi.org/10.1016/j.foodchem.2017.09.014.

42. Martínez-Sanz Marta, Fabra María José, Gómez-Mascaraque Laura G, López-Rubio Amparo: **Structural effects of microalgae additives on the starch gelatinisation process**. *Food Hydrocolloids* 2018, **77**:257–269, https://doi.org/10.1016/j.foodhyd.2017.10.002.

43. Hong J, Zeng X, Buckow R, Han Z, Wang M: **Nanostructure , morphology and functionality of cassava starch after pulsed electric fields assisted acetylation**. *Food Hydrocolloids* 2016, **54**:139–150, https://doi.org/10.1016/j.foodhyd.2015.09.025.

44. Zeng F, Gao Q, Han Z, Zeng X, Yu S: **Structural properties and digestibility of pulsed electric field treated waxy rice starch**. *Food Chem* 2016, **194**:1313–1319, https://doi.org/10.1016/j.foodchem.2015.08.104.

45. Liu X, Xiao X, Liu P, Yu L, Li M, Zhou S: **Shear degradation of corn starches with different amylose contents**. *Food Hydrocolloids* 2017, **66**:199–205, https://doi.org/10.1016/j.foodhyd.2016.11.023.

46. Niu M, Zhang B, Jia C, Zhao S: **Multi-scale structures and pasting characteristics of starch in whole-wheat flour treated by superfine grinding**. *Int J Biol Macromol* 2017, **104**:837–845, https://doi.org/10.1016/j.ijbiomac.2017.06.125.

47. Xiao L, Chen J, Wang X, Bai R, Chen D, Liu J: **Structural and physicochemical properties of chemically modified Chinese water chestnut [Eleocharis dulcis (Burm. f.) Trin. ex Hensch] starches**. *Int J Biol Macromol* 2018, **120**:547–556, https://doi.org/10.1016/j.ijbiomac.2018.08.161.

48. Doutch J, Bason M, Franceschini F, James K, Clowes D, Gilbert EP: **Structural changes during starch pasting using simultaneous Rapid Visco Analysis and small-angle neutron scattering**. *Carbohydr Polym* 2012, **88**:1061–1071, https://doi.org/10.1016/j.carbpol.2012.01.066.

49. Yang Z, Gu Q, Lam E, Tian F, Chaieb S, Hemar Y: **In situ study starch gelatinization under ultra-high hydrostatic pressure using synchrotron SAXS**. *Food Hydrocolloids* 2016, **56**:58–61, https://doi.org/10.1016/j.foodhyd.2015.12.007.

50. Blazek J, Gilbert EP: **Effect of enzymatic hydrolysis on native starch granule structure**. *Biomacromolecules* 2010:3275–3289.

51. Chen P, Xie F, Zhao L, Qiao Q, Liu X: **Effect of acid hydrolysis on the multi-scale structure change of starch with different amylose content**. *Food Hydrocolloids* 2017, **69**:359–368, https://doi.org/10.1016/j.foodhyd.2017.03.003.

52. Chen P, Wang K, Kuang Q, Zhou S, Wang D, Liu X: **Understanding how the aggregation structure of starch affects its gastrointestinal digestion rate and extent**. *Int J Biol Macromol* 2016, **87**:28–33, https://doi.org/10.1016/j.ijbiomac.2016.01.119.

53. Yang Z, Xu X, Singh R, Campo L De, Gilbert EP, Wu Z: **Effect of amyloglucosidase hydrolysis on the multi-scale supramolecular structure of corn starch**. *Carbohydr Polym* 2019, **212**:40–50, https://doi.org/10.1016/j.carbpol.2019.02.028.

54. * Martínez-Sanz M, Gidley MJ, Gilbert EP: **Application of X-ray and neutron small angle scattering techniques to study the hierarchical structure of plant cell walls : a review**. *Carbohydr Polym* 2015, **125**:120–134, https://doi.org/10.1016/j.carbpol.2015.02.010.
A review of the use of SAS to Plant Cell Wall materials with particular focus on cellulose.

55. Martínez-Sanz M, Gidley MJ, Gilbert EP: **Hierarchical architecture of bacterial cellulose and composite plant cell wall polysaccharide hydrogels using small angle neutron scattering †**. *Soft Matter* 2016:1534–1549, https://doi.org/10.1039/C5SM02085A.

56. Martínez-Sanz M, Mikkelsen D, Flanagan B, Gidley MJ, Gilbert EP: **Multi-scale model for the hierarchical architecture of native cellulose hydrogels**. *Carbohydr Polym* 2016, **147**:542–555, https://doi.org/10.1016/j.carbpol.2016.03.098.

57. Martínez-Sanz M, Mikkelsen D, Flanagan BM, *et al.*: **Investigation of the micro- and nano-scale architecture of cellulose hydrogels with plant cell wall polysaccharides : a combined USANS/SANS study**. *Polymer (Guildf)* 2016, **105**:449–460, https://doi.org/10.1016/j.polymer.2016.07.015.

58. Martínez-Sanz M, Mikkelsen D, Flanagan BM, Gidley MJ, Gilbert EP: **Multi-scale characterisation of deuterated cellulose composite hydrogels reveals evidence for different interaction mechanisms with arabinoxylan, mixed-linkage glucan and xyloglucan**. *Polymer (Guildf)* 2017, **124**:1–11, https://doi.org/10.1016/j.polymer.2017.07.036.

59. Liu D, Lopez-Sanchez P, Martinez-Sanz M, Gilbert EP, Gidley MJ: **Adsorption isotherm studies on the interaction between polyphenols and apple cell walls: effects of variety, heating and drying**. *Food Chem* 2019, **282**(January):58–66, https://doi.org/10.1016/j.foodchem.2018.12.098.

60. Lopez-Sanchez P, Martínez-Sanz M, Bonilla MR, *et al.*: **Pectin impacts cellulose fibre architecture and hydrogel mechanics in the absence of calcium**. *Carbohydr Polym* 2016, **153**:236–245, https://doi.org/10.1016/j.carbpol.2016.07.113.

61. Lopez-Sanchez P, Martínez-Sanz M, Bonilla MR, *et al.*: **Cellulose-pectin composite hydrogels : intermolecular interactions and material properties depend on order of assembly**. *Carbohydr Polym* 2017, **162**:71–81, https://doi.org/10.1016/j.carbpol.2017.01.049.

62. Liu D, Martínez-Sanz M, Lopez-Sanchez P, Gilbert EP, Gidley MJ: **Adsorption behaviour of polyphenols on cellulose is affected by processing history**. *Food Hydrocolloids* 2017, **63**:496–507, https://doi.org/10.1016/j.foodhyd.2016.09.012.

63. Schuster E, Wallin P, Klose FP, Gold J, Ström A: **Correlating network structure with functional properties of capillary alginate gels for muscle fiber formation**. *Food Hydrocolloids* 2017, https://doi.org/10.1016/j.foodhyd.2017.05.036.

64. Yu L, Yakubov GE, Martínez-Sanz M, Gilbert EP, Stokes JR: **Rheological and structural properties of complex arabinoxylans from Plantago ovata seed mucilage under non-gelled conditions**. *Carbohydr Polym* 2018, **193**(March):179–188.

65. Maki Y, Furusawa K, Dobashi T, Sugimoto Y, Wakabayashi K: **Small-angle X-ray and light scattering analysis of multi-layered Curdlan gels prepared by a diffusion method**. *Carbohydr Polym* 2017, **155**:136–145, https://doi.org/10.1016/j.carbpol.2016.08.061.

66. Lopez-Rubio Amparo, Tarancón Paula, Gómez-Mascaraque Laura G, Martínez-Sanz Marta, Fabra Maria Jose, Martínez Juan Carlos, Fiszman Susana: **Development of glucomannan-chitosan interpenetrating hydrocolloid networks (IHNs) as a potential tool for creating satiating ingredients**. *Food Hydrocolloids* 2016, **60**:533–542, https://doi.org/10.1016/j.foodhyd.2016.04.033.

67. Morishima K, Nakamura N, Matsui K, *et al.*: **Formation of clusters in whiskies during the maturation process**. *J Food Sci* 2019, https://doi.org/10.1111/1750-3841.14398.

68. Urade R: **Gliadins from wheat grain: an overview, from primary structure to nanostructures of aggregates**. *Biophys Rev* 2018, **10**:435–443.

69. Xiao J, Shi C, Zhang L, *et al.*: **Multilevel structural responses of β-conglycinin and glycinin under acidic or alkaline heat treatment**. *FRIN* 2016, **89**:540–548, https://doi.org/10.1016/j.foodres.2016.09.006.

70. Gupta R, Hogan CJ, Perugini MA, Soares TP: **Characterization of recombinant dihydrodipicolinate synthase from the bread wheat Triticum aestivum**. *Planta* 2018, **248**:381–391, https://doi.org/10.1007/s00425-018-2894-x.

71. Rasheed S, Ahmad S, Falke S, *et al.*: **Isolation and initial structural characterization of a 27 kDa protein from Zingiber officinale**. *J Mol Struct* 2018, **1156**:330–335, https://doi.org/10.1016/j.molstruc.2017.11.116.

72. Sun Y, Oseliero PL, Oliveira CLP: **α-Lactalbumin and sodium dodecyl sulfate aggregates: denaturation, complex formation and time stability**. *Food Hydrocolloids* 2017, **62**:10–20, https://doi.org/10.1016/j.foodhyd.2016.07.031.

73. ** De Kruif CG, Huppertz T, Urban VS, Petukhov AV: **Casein micelles and their internal structure**. *Adv Colloid Interface Sci* 2012, **171–172**:36–52, https://doi.org/10.1016/j.cis.2012.01.002.
A comprehensive review of all SAS studies on casein micelles and the controversy concerning their internal structure.

74. ** Ingham B, Erlangga GD, Smialowska A, *et al.*: **Solving the mystery of the internal structure of casein micelles**. *Soft Matter* 2015, **11**:2723–2725, https://doi.org/10.1039/C5SM00153F.
Resonant soft X-ray SAXS at the calcium absorption edge is used to verify the origin of controversial peak observed in SAS studies as arising from the separation of colloidal calcium phosphate particles.

75. Ingham B, Smialowska A, Erlangga GD, *et al.*: **Revisiting the interpretation of casein micelle SAXS data**. *Soft Matter* 2016, **12**:33–38, https://doi.org/10.1039/c6sm01091a.

76. Mata JP, Udabage P, Gilbert EP: **Structure of casein micelles in milk protein concentrate powders via small**. *Soft Matter* 2011, **7**:3837–3843, https://doi.org/10.1039/c0sm01010c.

77. Ingham B, Kirby N, Wang C, Carr A: **Elemental fingerprinting of mineral species in iron-fortified milk : anomalous small-angle X-ray scattering and resonant soft X-ray scattering studies research papers**. *J Synchrotron Radiat* 2018, **25**:1106–1112, https://doi.org/10.1107/S1600577518007774.

78. Ingham B, Smialowska A, Kirby NM, Wang C, Carr AJ: **A structural comparison of casein micelles in cow, goat and sheep milk using X-ray scattering**. *Soft Matter* 2018, https://doi.org/10.1039/c8sm00458g.

79. Day L, Raynes JK, Leis A, Liu LH, Williams RPW: **Probing the internal and external micelle structures of differently sized casein micelles from individual cows milk by dynamic light and small-angle X-ray scattering**. *Food Hydrocolloids* 2017, **69**:150–163, https://doi.org/10.1016/j.foodhyd.2017.01.007.

80. Yang Z, Gu Q, Banjar W, Li N, Hemar Y: **In situ study of skim milk structure changes under high hydrostatic pressure using synchrotron SAXS**. *Food Hydrocolloids* 2018, **77**:772–776, https://doi.org/10.1016/j.foodhyd.2017.11.019.

81. Lam E, Holt C, Edwards P, *et al.*: **The effect of transglutaminase treatment on the physico-chemical properties of skim milk with added ethylenediaminetetraacetic acid**. *Food Hydrocolloids* 2017, **69**, https://doi.org/10.1016/j.foodhyd.2017.02.002.

82. Li Z, Yang Z, Otter D, *et al.*: **Rheological and structural properties of coagulated milks reconstituted in D_2O: comparison between rennet and a tamarillo enzyme (tamarillin)**. *Food Hydrocolloids* 2018, **79**:170–178, https://doi.org/10.1016/j.foodhyd.2017.12.004.

83. Kuo W, Ilavsky J, Lee Y: **Structural characterization of solid lipoproteic colloid gels by ultra-small-angle X-ray scattering and the relation with sodium release**. *Food Hydrocolloids* 2016, **56**:325–333, https://doi.org/10.1016/j.foodhyd.2015.12.032.

84. Smialowska A, Matia-Merino L, Ingham B, Carr AJ: **Effect of calcium on the aggregation behaviour of caseinates**. *Colloids Surfaces A Physicochem Eng Asp* 2017, **522**:113–123, https://doi.org/10.1016/j.colsurfa.2017.02.074.

85. Huck-Iriart Cristián, Montes-de-Oca-Ávalos Juan, Herrera María Lidia, Candal Roberto Jorge, Pinto-de-Oliveira Cristiano Luis, Linares-Torriani Iris: **New insights about flocculation process in sodium caseinate-stabilized emulsions**. *Food Res Int* 2016, **89**:338–346, https://doi.org/10.1016/j.foodres.2016.08.026.

86. Montes-de-Oca-Ávalos Juan, Huck-Iriart Cristián, Candal RJ: **Sodium caseinate/sunflower oil emulsion-based gels for structuring food**. *Food Bioprocess Technol* 2016, **9**:981–992, https://doi.org/10.1007/s11947-016-1687-0.

87. Araujo R, Fattori J, Michelon M, Lopes R: **Formation and pH-stability of whey protein fibrils in the presence of lecithin**. *Food Hydrocolloids* 2016, **60**:288–298, https://doi.org/10.1016/j.foodhyd.2016.03.039.

88. Hoban JM, Hopkins DL, Kirby N, *et al.*: **Application of small angle X-ray scattering synchrotron technology for measuring ovine meat quality**. *Meat Sci* 2016, https://doi.org/10.1016/j.meatsci.2016.03.005.

89. Hughes J, Clarke F, Li Y, Purslow P, Warner R: **Differences in light scattering between pale and dark beef longissimus thoracis muscles are primarily caused by differences in the myofilament lattice, myofibril and muscle fibre transverse spacings**. *Meat Sci* 2019, https://doi.org/10.1016/j.meatsci.2018.11.006.

90. Liu J, Schwartzkopf M, Arner A: **Rigor bonds cause reduced sarcomeric volume in skinned porcine skeletal muscle under PSE-like conditions**. *Meat Sci* 2018, https://doi.org/10.1016/j.meatsci.2018.01.014.

91. Yang Z, Hemar Y, Hilliou L, *et al.*: **Nonlinear behavior of gelatin networks reveals a hierarchical structure**. *Biomacromolecules* 2016, **17**(2):590–600, https://doi.org/10.1021/acs.biomac.5b01538.

92. Xu AY, Melton LD, Ryan TM, *et al.*: **Sugar-coated proteins: the importance of degree of polymerisation of oligo-galacturonic acid on protein binding and aggregation**. *Soft Matter* 2017, **13**:2698–2707, https://doi.org/10.1039/c6sm02660e.

93. Xu AY, Melton LD, Ryan TM, *et al.*: **Effects of polysaccharide charge pattern on the microstructures of b-lactoglobulin-pectin complex coacervates, studied by SAXS and SANS**. *Food Hydrocolloids* 2018, **77**:952–963, https://doi.org/10.1016/j.foodhyd.2017.11.045.

94. Atay E, Jose M, Martínez-sanz M, Gomez-mascaraque LG, Altan A, Lopez-rubio A: **Development and characterization of chitosan/gelatin electrosprayed microparticles as food grade delivery vehicles for anthocyanin extracts**. *Food Hydrocolloids* 2018, **77**:699–710, https://doi.org/10.1016/j.foodhyd.2017.11.011.

95. Shi C, Tang H, Xiao J, *et al.*: **Small-angle X-ray scattering study of protein complexes with tea polyphenols**. *J Agric Food Chem* 2017, **65**:656–665, https://doi.org/10.1021/acs.jafc.6b04630.

96. Benito-González I, López-Rubio A, Martínez-Sanz M: **Potential of lignocellulosic fractions from Posidonia oceanica to improve barrier and mechanical properties of bio-based packaging materials**. *Int J Biol Macromol* 2018, **118**:542–551, https://doi.org/10.1016/j.ijbiomac.2018.06.052.

97. Corsello FA, Bolla PA, Anbinder PS, Serradell MA, Amalvy JI, Peruzzo PJ: **Morphology and properties of neutralized chitosan-cellulose nanocrystals biocomposite films**. *Carbohydr Polym* 2017, **156**:452–459, https://doi.org/10.1016/j.carbpol.2016.09.031.

98. Fabra MJ, Martínez-Sanz M, Gavara R: **Structural and physicochemical characterization of thermoplastic corn starch fi lms containing microalgae**. *Carbohydr Polym* 2018, **186**:184–191, https://doi.org/10.1016/j.carbpol.2018.01.039.

99. Romani VP, Machado AV, Olsen BD, Martins VG: **Effects of pH modification in proteins from fish (Whitemouth croaker) and their application in food packaging films**. *Food Hydrocolloids* 2018, **74**:307–314, https://doi.org/10.1016/j.foodhyd.2017.08.021.

100. Sieg H, Ka C, Bo L, *et al.*: **Impact of an artificial digestion procedure on aluminum-containing nanomaterials**. *Langmuir* 2017, **33**:10726–10735, https://doi.org/10.1021/acs.langmuir.7b02729.

101. Kästner C, Lichtenstein D, Lampen A, Thünemann AF: **Monitoring the fate of small silver nanoparticles during artificial digestion**. *Colloids Surface A Physicochem Eng Asp* 2017, **526**:76–81, https://doi.org/10.1016/j.colsurfa.2016.08.013.

102. Chatzidaki MD, Papadimitriou K, Alexandraki V, *et al.*: **Reverse micelles as nanocarriers of nisin against foodborne pathogens**. *Food Chem* 2018, https://doi.org/10.1016/j.foodchem.2018.02.053.

103. Gilbert EP: **Neutrons and food: barriers and opportunities**. *Neutron News* 2012;(May):37–41.